

Mechanistic Insights into Copper-Catalyzed Michael Reactions

Elisabet Pérez,^[a,b] Marcial Moreno-Mañas,^{[b]†} Rosa María Sebastián,^[b]
Adelina Vallribera,^{*[b]} and Anny Jutand^{*[a]}

Keywords: Copper / Michael addition / Reaction mechanisms

The mechanism of the Michael reaction between 2-(ethoxy-carbonyl)cyclopentanone (**2**) and methyl vinyl ketone (**3**) catalyzed by the copper(II) salt [Cu(5-*t*Bu-Sal)₂] (**1**) has been investigated in toluene. The kinetics of the reaction of the catalyst **1** with the oxo ester **2** has been investigated by UV/Vis spectroscopy. It has been established that [Cu(5-*t*Bu-Sal)₂] (**1**) reacts with **2** in a first-order reaction, which is retarded by 5-*t*Bu-Sal-H (**6**), formed in the reaction after the reversible dissociation of [Cu(5-*t*Bu-Sal)₂] to [Cu(5-*t*Bu-Sal)]⁺ and 5-

*t*Bu-Sal⁻ and the subsequent reversible deprotonation of **2** by 5-*t*Bu-Sal⁻. The formation of the mixed complex [Cu(5-*t*Bu-Sal)(enolate-**2**)] (**5**) is proposed and has been characterized by cyclic voltammetry. The rate constant for the overall reaction leading to [Cu(5-*t*Bu-Sal)(enolate-**2**)] (**5**) has been determined. The reaction of the mixed complex **5** with methyl vinyl ketone (**3**), investigated by cyclic voltammetry, is proposed as the rate-determining step.

Introduction

The Michael addition of active methylene compounds to activated π systems is one of the most powerful tools for C–C bond formation.^[1] Catalysis by transition metals or lanthanides is an important alternative to the use of bases.^[2] Among transition metals, copper is probably the metal that has attracted most attention as a catalyst in Michael reactions since the pioneering work of Saegusa and Nelson and their co-workers, who described the combination of isocyanides and Cu₂O or Cu(acac)₂,^[3] or Cu(baen)^[4] [the copper(II) complex of the product formed by the Schiff base condensation of 2,4-pentanedione with ethylenediamine]. Since then, several groups have studied enantioselective Michael additions. Christoffers and co-workers proposed the use of Co(OAc)₂·H₂O and α -amino acid amides as chiral auxiliaries [including their immobilization in poly(ethylene glycol)], obtaining excellent *ees* in the reactions of enantiopure enamines of β -dicarbonyl compounds with methyl vinyl ketone as electrophile.^[5] A different approach was adopted by Jørgensen and co-workers, who used the combination of Cu(OTf)₂ and chiral bis(oxazolines) in the reactions of open and cyclic oxo esters with azodicarboxylates.^[6] More recently, a camphor-derived acrylate equiva-

lent has been used by Palomo et al. as a chiral acrylate in copper-catalyzed reactions of β -oxo esters.^[7] Copper triflate/[bmim]BF₄ has been recommended for good recycling of the catalyst.^[8]

Some of us have previously reported that Ni(salicylaldehyde)₂·2H₂O [Ni(sal)₂·2H₂O] is an efficient catalyst for the reactions of a series of Michael acceptors and 3-methyl-2,4-pentadione and ethyl 2-methyl-3-oxobutanoate with the generation of quaternary centers.^[9] Furthermore, some of these reactions were performed under organic perfluorinated biphasic conditions using a nickel(II) complex of the Schiff base of salicylaldehyde and 4-(perfluorodecyl)-aniline. The perfluorinated phase, in which the catalyst is soluble, was reused in four consecutive reactions without loss of activity.^[10] We have also been interested in the diastereoselective metal-catalyzed Michael addition reactions of *N*-acetoacetic and 3-oxostearic acid derivatives of enantiomerically pure common chiral auxiliaries, a method that has been applied with success to the synthesis of enantiopure *syn*-1,2-hydrazino alcohols.^[11] In addition, we have compared the activity of different transition metals and came to the conclusion that the copper(II) complex of salicylaldehyde is slightly better than [Ni(sal)₂·2H₂O]. To improve the solubility in organic solvents we introduced a *tert*-butyl group onto the aromatic ring. Thus, complex [Cu(5-*t*Bu-Sal)₂] (**1**) catalyzed the Michael reaction of 2-(ethoxy-carbonyl)cyclopentanone (**2**) with butenone (**3**), ethyl acrylate, acrylonitrile, and diethyl azodicarboxylate. One serious limitation of many metal species is that their catalytic activity is limited to very active Michael acceptors (unsaturated ketones and dialkyl azodicarboxylates), other acceptors such as acrylates and acrylonitrile being inactive.

[a] Ecole Normale Supérieure, Département de Chimie, UMR CNRS-ENS-UPMC 8640, 24 Rue Lhomond, 75231 Paris Cedex 5, France
Fax: +33-1-44322402
E-mail: Anny.Jutand@ens.fr

[b] Department of Chemistry, Universitat Autònoma de Barcelona, 08193 Cerdanyola del Vallès, Barcelona, Spain
Fax: +34-93-5811265
E-mail: adelina.vallribera@uab.es

[†] Deceased on February 20, 2006

Although the usefulness of the Michael reaction has been widely demonstrated, experiments have so far provided limited insight into the mechanism. In particular, for the above-mentioned reaction, a catalytic cycle based on the results of IR and UV/Vis spectroscopy and GLC analysis was proposed for this reaction (Scheme 1).^[12] The catalytic cycle starts from complex **1**, and we assume the formation of intermediate **5** and free 5-*tert*-butylsalicylaldehyde (**6**) by an exchange of Cu ligands. Evidence for the formation of complex **5** was indirectly obtained by identification of 5-*tert*-butylsalicylaldehyde (**6**) by IR spectroscopy (1655 cm⁻¹) and GLC analysis of the reaction mixture of **1** and **2** (molar ratio 1:2). Moreover, we undertook a preliminary UV/Vis spectroscopic study of the interactions of covalent catalyst **1** with the components of the reaction of **2** and **3**. We determined that β -oxo ester **2** interacts with copper complex **1**, as shown by the bathochromic displacement (in dichloromethane) of the bands in the UV/Vis spectrum of copper complex **1** upon mixing **1** with **2**. No significant interaction between **1** and **3** was detected in that UV/Vis region. These results suggest the in situ generation of some active species with the general structures of **5** and/or **7**, which should both

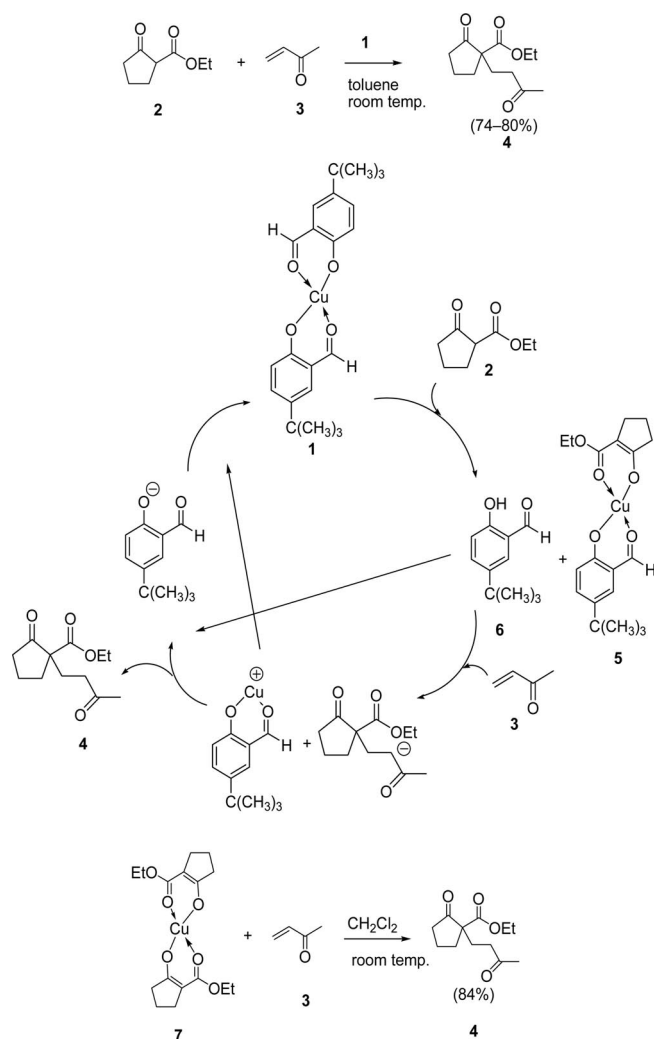
react in a similar way. In fact, the copper enolate **7**, independently prepared from β -oxo ester **2** and Cu(OAc)₂,^[12] reacts with butenone (**3**) to afford the Michael adduct **4** in 84% yield (Scheme 1). Complex **7** is formed by ligand exchange of Cu complex **5** in the presence of β -oxo ester **2** at room temp. over a long period of time.

To obtain more insight into the proposed steps and intermediates of the mechanism for the reaction of the oxo ester **2** with 2-butenone (**3**) catalyzed by [Cu(5-*t*Bu-Sal)₂] (Scheme 1), the kinetics of the first steps of the catalytic cycle have been investigated by UV spectroscopy and electrochemical techniques.

Results and Discussion

Mechanism of the Reaction of [Cu(5-*t*Bu-Sal)₂] (**1**) with the Oxo Ester **2**, as Monitored by UV Spectroscopy

All experiments were performed in toluene at 30 °C. [Cu(5-*t*Bu-Sal)₂] (**1**; *c*₀ = 0.706 mM) exhibited an absorption band at λ_{max} = 397 nm (Figure 1). When reagents **2** (20 equiv.) and **3** (100 equiv.) were added to a fresh solution of [Cu(5-*t*Bu-Sal)₂] (**1**; 2 mM) in toluene, the UV band of **1** disappeared within 10 min. A new UV band was observed at λ_{max} = 423 nm, the absorbance of which was almost constant within 4 h. After 5 h (corresponding to the end of the catalytic reaction), the UV band of complex **1** was restored (Figure 2), albeit with decreased absorbance. Thus, [Cu(5-*t*Bu-Sal)₂] (**1**) disappeared in a fast reaction in the presence of the reagents and did not accumulate in the catalytic reaction. It was readily transformed into another Cu complex, the concentration of which was almost constant during the catalytic reaction. This intermediate Cu complex accumulated (resting state) and was thus involved in the rate-determining step of the catalytic reaction. Its structure should not differ too much from that of the initial catalyst **1** because their respective maximum wavelengths are close to each other (423 vs. 397 nm).



Scheme 1. Previously suggested catalytic cycle for catalyst **1**.

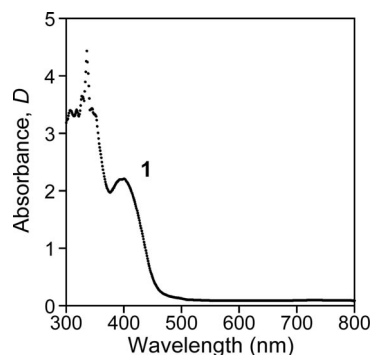


Figure 1. UV spectrum of [Cu(5-*t*Bu-Sal)₂] (**1**; 0.706 mM) in toluene in a 1 cm pathlength cell at 30 °C.

UV spectral analysis of a fresh solution of [Cu(5-*t*Bu-Sal)₂] (**1**; 0.73 mM) after given periods of time revealed that its absorbance slowly decreased with time: 13% lower after

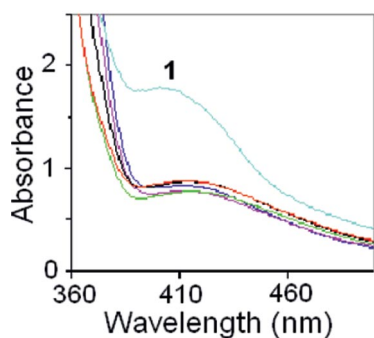


Figure 2. Evolution with time of the UV spectrum of $[\text{Cu}(5\text{-}t\text{Bu-Sal)}_2]$ (**1**; 2 mM) in toluene in a 1 cm pathlength cell at 30 °C after addition of a mixture of **2** (20 equiv.) and **3** (100 equiv.). The dark-blue, pink, black, green, and red UV spectra were recorded after 10 min, 1, 2, 3, and 4 h, respectively. The upper turquoise UV spectrum, which characterizes complex **1**, was recorded after 5 h.

4 h and 21% lower after 20 h, attesting to a slow decomposition of **1**. Kinetic measurements of the reaction of **1** with the oxo ester **2** could thus be investigated within 4 h without a significant contribution from the decomposition of **1**. The kinetics of the reaction of complex **1** (0.7 mM) with the oxo ester **2** was monitored by UV spectroscopy by recording the decrease in its absorbance D ($D_0 = 1.7$), measured at $\lambda_{\text{max}} = 397$ nm, with time after the addition of the oxo ester **2** (20, 30, 40, and 50 equiv.; Figure 3). In all cases, the final absorbance was low ($D_{\text{final}} \approx 0.25$) and almost constant, attesting to an irreversible reaction between **1** and **2**.

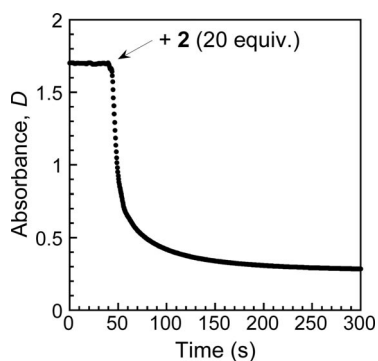


Figure 3. Variation of the UV absorbance at $\lambda = 397$ nm of $[\text{Cu}(5\text{-}t\text{Bu-Sal)}_2]$ (**1**; 0.7 mM) in toluene after the addition of **2** (20 equiv.) at 30 °C.

The plot of $\ln x$ against time was not linear throughout the reaction and for all concentrations of the oxo ester **2** [x = molar fraction of **1**, $x = (D_t - D_{\text{final}})/(D_0 - D_{\text{final}})$, in which D_t = absorbance at time t , D_0 = initial absorbance, and D_{final} = absorbance at the end of the reaction; Figure 4]. The kinetic curve may be divided into two parts: Part I at short reaction times ($\ln x = -k^{\text{I}}_{\text{obs}}t$), which characterizes the reaction up to 50% conversion, and Part II at longer reaction times, beyond 80% conversion ($\ln x = -k^{\text{II}}_{\text{obs}}t$) when the disappearance of $[\text{Cu}(5\text{-}t\text{Bu-Sal)}_2]$ (**1**) was slower (Figure 4). The plot of $k^{\text{I}}_{\text{obs}}$ against the concentra-

tion of **2** was linear, attesting to a first-order reaction in the oxo ester **2**: $k^{\text{I}}_{\text{obs}} = k^{\text{I}}[\mathbf{2}]$ with $k^{\text{I}} = 8.9 \text{ M}^{-1} \text{ s}^{-1}$ (toluene, 30 °C; Figure 5).^[13]

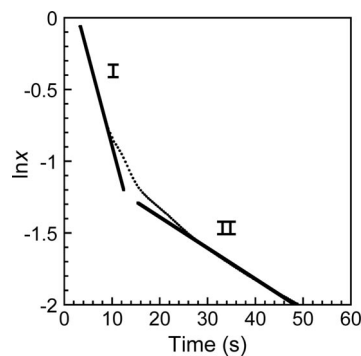


Figure 4. Kinetics of the reaction of $[\text{Cu}(5\text{-}t\text{Bu-Sal)}_2]$ (**1**; 0.73 mM) and the oxo ester **2** (20 equiv.) in toluene at 30 °C. x = molar fraction of **1**.

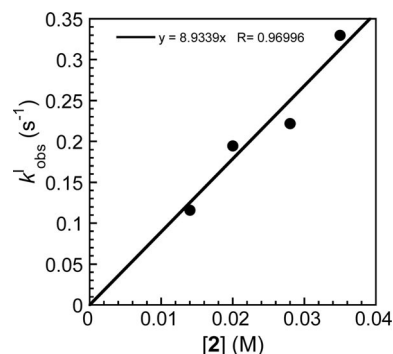


Figure 5. Determination of the reaction order for the oxo ester **2** in its reaction with $[\text{Cu}(5\text{-}t\text{Bu-Sal)}_2]$ (**1**; 0.7 mM) in toluene at 30 °C. $k^{\text{I}}_{\text{obs}}$ was determined from the slope of the straight line at short reaction times (Part I), as in Figure 4, for different concentrations of **2**.

For simplification, $[\text{Cu}(5\text{-}t\text{Bu-Sal)}_2]$ (**1**) was expressed as CuA_2 and the oxo ester **2** as BH. The reaction of neutral CuA_2 with BH cannot proceed directly because acid/base reactions must be involved. The neutral complex CuA_2 is partly dissociated in solution to CuA^+ and A^- . Indeed, the absorbance of CuA_2 increased upon successive addition of AH (**6**, 5-*tert*-butylsalicylaldehyde) that is, successive addition of A^- (Figure 6). These results suggest that CuA^+ is involved in the catalytic cycle through Equilibrium (1) in Scheme 2.

According to the proposed mechanism displayed in Scheme 2, Part I in Figure 4 would be represented by Equations (1)–(3), and Part II by Equations (4) and (5), in which some CuA_2 would be regenerated from the formation of AH in Equation (2). The kinetic law corresponding to Equations (1)–(3) is displayed in Scheme 3.

The kinetic law in Equation (7) reveals a first-order reaction for BH (**2**), which was found experimentally (Figure 5), and a reaction order of -1 for AH. The experiments shown in Figure 4 were conducted in the absence of added AH. AH was generated in Equation (2) at a concentration that varied throughout the reaction. To confirm the kinetic law,

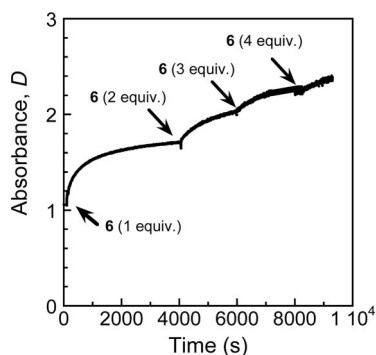
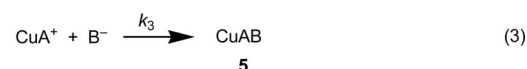
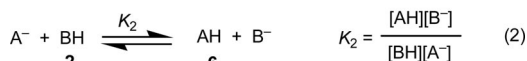
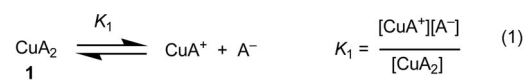
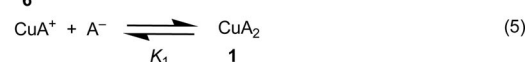


Figure 6. Evolution of the UV absorbance at $\lambda = 397$ nm of $[\text{Cu}(5\text{-}t\text{Bu-Sal})_2]$ (**1**; 0.53 mM) in toluene in a 1 cm pathlength cell at 30 °C in the presence of **6** as indicated by the arrows (total number of equiv. of **6**).



At longer times:



Scheme 2.

$$\text{rate} = k_3[\text{B}^-][\text{CuA}^+]$$

$$[\text{Cu}] = [\text{CuA}^+] + [\text{CuA}_2] = [\text{CuA}^+] + [\text{CuA}^+][\text{A}^-]/K_1 = [\text{CuA}^+](1 + [\text{A}^-]/K_1)$$

$$d[\text{Cu}]/dt = -k_3[\text{B}^-][\text{Cu}]/(1 + [\text{A}^-]/K_1)$$

$$\text{If } [\text{A}^-]/K_1 \gg 1, \text{ then } d[\text{Cu}]/dt = -k_3K_1[\text{B}^-][\text{Cu}]/[\text{A}^-] = -k_3K_1K_2[\text{Cu}][\text{BH}]/[\text{AH}]$$

$$d[\text{Cu}]/[\text{Cu}] = \frac{-k_3K_1K_2[\text{BH}]dt}{[\text{AH}]} \quad (6)$$

Integration of Eq. (6) gives Eq. (7)

if BH and AH are in large excess (> 10 equiv.)

$$\ln x = \frac{-k_3K_1K_2[\text{BH}]t}{[\text{AH}]} \quad (7)$$

Scheme 3.

the disappearance of **1** (CuA_2) in its reaction with **2** (BH) was studied in the presence of excess AH (**6**). Compound **6** (5 equiv.) was first added to $[\text{Cu}(5\text{-}t\text{Bu-Sal})_2]$ (**1**; $c_0 = 0.25$ mM), the absorbance of which at $\lambda = 397$ nm increased with time (Figure 7), in agreement with the experiments shown in Figure 6. The oxo ester **2** (20 equiv.) was then introduced after the absorbance had reached a constant value (Figure 7), and the absorbance of **1** dropped to its final value, as observed in the absence of added AH (Figure 3).

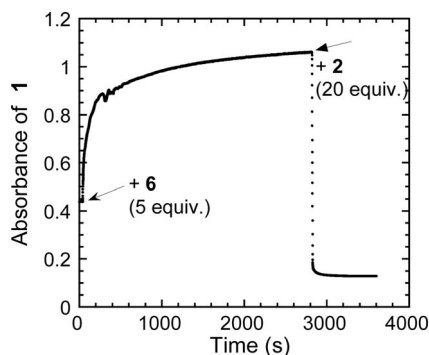


Figure 7. Evolution of the UV absorbance at $\lambda = 397$ nm of $[\text{Cu}(5\text{-}t\text{Bu-Sal})_2]$ (**1**; 0.25 mM) in toluene in a 1 cm pathlength cell at 30 °C after the addition of **6** (5 equiv.). The oxo ester **2** (20 equiv.) was added after 2800 s, as indicated by the arrow.

The kinetics of the latter reaction was investigated by plotting $6\ln x - x + 1$ vs. time [$x = [\text{I}]_t/[\text{I}]_0$ in the presence of **6**, $x = (D_t - D_{\text{final}})/(D_0 - D_{\text{final}})$, in which D_t = absorbance at time t , D_0 = initial absorbance, and D_{final} = absorbance at the end of the reaction]. The plot was linear up to 65% conversion (Figure 8), in agreement with the theoretical kinetic law obtained when **6** (5 equiv.) was added. The kinetic law $6\ln x - x + 1 = -k_3K_1K_2[\text{BH}]t/C_0$ was obtained by integration of Equation (6) in Scheme 3, in which $[\text{AH}] = c_0(6 - x)$. From the slope of the straight line, one determines $k_3K_1K_2 = 0.063 \text{ s}^{-1}$ (toluene, 30 °C). This was further confirmed when the same reaction was performed by adding 10 equiv. of **6** to **1** before the oxo ester **2** (20 equiv.). Indeed, a similar value was found ($k_3K_1K_2 = 0.051 \text{ s}^{-1}$) from the slope of the straight line obtained by plotting $\ln x$ vs. time [Equation (7)] up to 50% conversion. Both experiments provide evidence that the reaction order for **6** is indeed -1 .

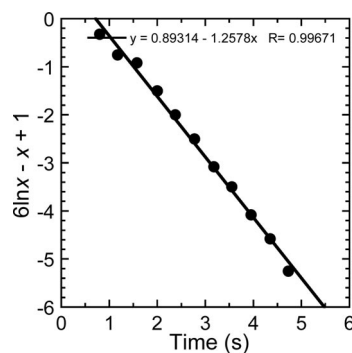


Figure 8. Kinetics of the reaction of $[\text{Cu}(5\text{-}t\text{Bu-Sal})_2]$ (**1**; 0.25 mM) with the oxo ester **2** (20 equiv.) in the presence of **6** (5 equiv.) added before **2** (see Figure 7) in toluene at 30 °C.

The reaction of $[\text{Cu}(5\text{-}t\text{Bu-Sal})_2]$ (**1**) with the oxo ester **2** was also monitored by cyclic voltammetry^[14] performed in acetonitrile (a solvent compatible with electrochemical experiments that is also a good solvent for Michael reactions).^[15] The cyclic voltammogram of **1** (2 mM) performed at a steady gold disk electrode exhibited a main irreversible reduction peak at $E_{\text{P,R}}^{\text{P}} = -0.53$ V vs. SCE followed by a

minor reduction peak at $E_{R2}^p = -0.89$ V (Figure 9). An oxidation peak observed on the reverse scan at $E_{O2}^p = -0.08$ V characterized a species generated at the second reduction peak, a “naked” Cu^0 adsorbed at the electrode, as illustrated in Figure 9. The mechanism for the electrochemical reduction of **1** is displayed in Scheme 4.

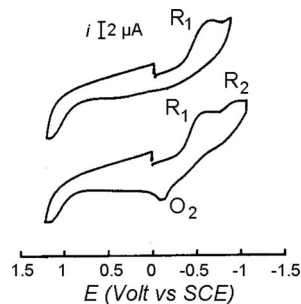
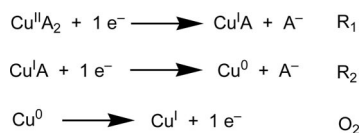


Figure 9. Cyclic voltammetry performed at a gold disk electrode ($d = 1$ mm) in acetonitrile containing $n\text{Bu}_4\text{NBF}_4$ (0.3 M) at a scan rate of 0.5 V s^{-1} at 22°C . Reduction of $[\text{Cu}(5\text{-}t\text{Bu-Sal})_2]$ (**1**; 2 mM).



Scheme 4.

AH (**6**) exhibited a single irreversible reduction peak at $E_{R3}^p = -1.75$ V. The oxo ester **2** was not electroactive in the investigated potential range (+0.5 to -2 V). The oxo ester **2** (1, 2, 3, 4, 10, and 20 equiv.) was added to $[\text{Cu}(5\text{-}t\text{Bu-Sal})_2]$ (**1**; 2 mM) in acetonitrile. A progressive decrease in the two successive reduction peaks of **1** was observed in the corresponding CVs, and they fully disappeared in the presence of 4 equiv. of **2** (Figure 10). Three new reduction peaks appeared at $E_{R4}^p = -1.18$ V, $E_{R5}^p = -1.61$ V, and $E_{R3}^p = -1.83$ V vs. SCE. The latter is close to the reduction peak of AH (**6**). This shows that a reaction between **1** and **2** took place that delivered AH [as proposed in Equation (2) of Scheme 2]. The oxidation peak at $E_{O2}^p = -0.08$ V, which characterizes the oxidation of an electrogenerated “naked” Cu^0 adsorbed at the electrode, was still observed in the reverse scan in the absence of complex **1** due to its reaction with the oxo ester **2** (Figure 10c). This indicates that the reduction process at R_4/R_5 generates “naked” Cu^0 . R_4 and R_5 are thus assigned to the reduction of the mixed complex CuAB (**5**) [Equation (3) in Scheme 2].

The further steps of the catalytic cycle were then investigated by adding methyl vinyl ketone (**3**; 1 equiv.) to CuAB (**5**), formed by treating **2** (4 equiv.) with $[\text{Cu}(5\text{-}t\text{Bu-Sal})_2]$ (**1**; 2 mM) in acetonitrile. The two reduction peaks R_1 and R_2 of $[\text{Cu}(5\text{-}t\text{Bu-Sal})_2]$ (**1**) were partly recovered (Figure 11), whereas the two reduction peaks R_4 and R_5 of CuAB (**5**) were still observed but at a lower intensity than in the absence of **3** (compare Figure 11 with Figure 10c).

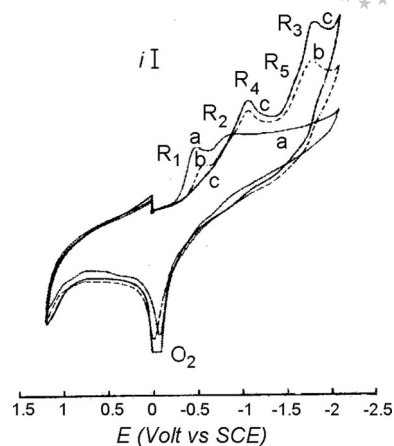


Figure 10. Cyclic voltammetry performed at a gold disk electrode ($d = 1$ mm) in acetonitrile containing $n\text{Bu}_4\text{NBF}_4$ (0.3 M) at a scan rate of 0.5 V s^{-1} at 22°C . (a): Reduction of $[\text{Cu}(5\text{-}t\text{Bu-Sal})_2]$ (**1**; 2 mM); (b): in the presence of **2** (4 mM); (c): in the presence of **2** (8 mM).

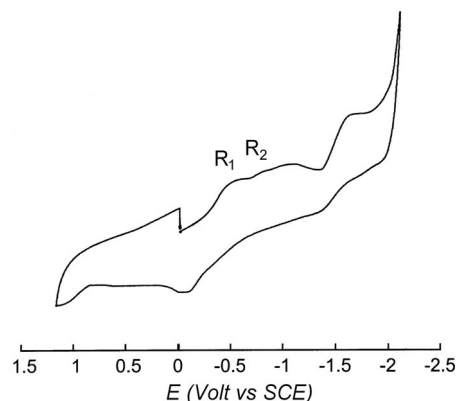
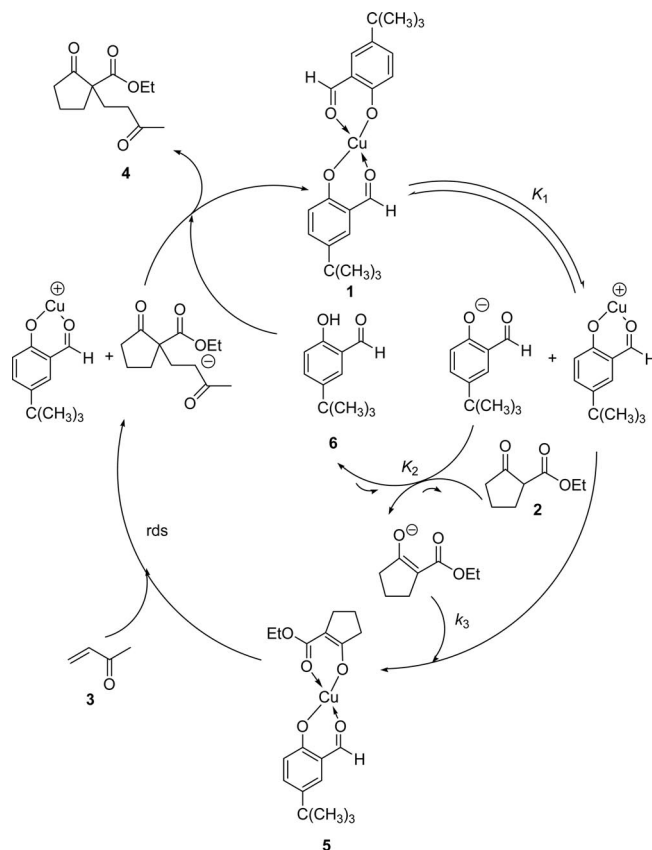


Figure 11. Cyclic voltammetry performed at a gold disk electrode ($d = 1$ mm) in acetonitrile containing $n\text{Bu}_4\text{NBF}_4$ (0.3 M) at a scan rate of 0.5 V s^{-1} at 22°C after the addition of **3** (2 mM) to CuAB (2 mM) generated in situ as in Figure 10c.

The reduction peak currents of R_1 and R_2 of **1** further increased upon the addition of a further 3 equiv. of **3** at the expense of the two reduction-peak currents of CuAB (**5**) at R_4 and R_5 . The reduction peak of AH (**6**) was no longer detected. These experiments provide evidence for the reaction of methyl vinyl ketone (**3**) with the intermediate complex CuAB (**5**), which restored the initial $[\text{Cu}(5\text{-}t\text{Bu-Sal})_2]$ (**1**). The disappearance of AH (**6**) indicates that a protonation reaction has occurred, as required for the formation of the Michael product **4**. Consequently, the first catalytic cycle has been closed. This also shows that the reaction of CuAB (**5**) with methyl vinyl ketone (**3**) is quite slow and suggests that the mixed complex **5** is involved in the rate-determining step of the catalytic cycle. Such a step was also observed by UV spectroscopy (Figure 2).

All the data obtained by UV/Vis and cyclic voltammetry studies allowed us to propose a new catalytic cycle for this reaction (Scheme 5). The rates and mechanism of the first three steps have been determined. Furthermore, the mixed complex $[\text{Cu}(5\text{-}t\text{Bu-Sal})(\text{enolate-2})]$ (**5**) appears to be the

key intermediate in the catalytic reaction and is involved in the rate-determining step. Similar complexes have previously been proposed for lanthanide-catalyzed Michael addition reactions.^[15]



Scheme 5.

Conclusions

The mechanism for the $[\text{Cu}(5\text{-}t\text{Bu-Sal})_2]$ -catalyzed Michael reaction has been investigated by UV/Vis spectroscopy and cyclic voltammetry. The rates and mechanism of the first three steps of the catalytic cycle have been characterized. $[\text{Cu}(5\text{-}t\text{Bu-Sal})_2]$ (**1**) reacts with the β -oxo ester **2** in a first-order reaction retarded by 5-*t*Bu-Sal-H. The reaction consists of a reversible dissociation of **1** to $[\text{Cu}(5\text{-}t\text{Bu-Sal})]^+$ and 5-*t*Bu-Sal⁻, followed by the deprotonation of **2** by 5-*t*Bu-Sal⁻ to form enolate-**2**, and the subsequent formation of the mixed complex $[\text{Cu}(5\text{-}t\text{Bu-Sal})(\text{enolate-2})]$ (**5**; Scheme 5). The rate constant for the overall formation of **5** was determined as $k_3K_1K_2$. The intermediate complex **5** was characterized by UV/Vis spectroscopy and cyclic voltammetry studies. It reacts with methyl vinyl ketone (**3**) to give the Michael product **4** in the rate-determining step (Scheme 5).

Experimental Section

General Methods: All experiments were performed by using standard Schlenk techniques under argon. UV/Vis spectra were re-

corded on an mc² Safas Monaco spectrometer. Cyclic voltammetry was performed with a home-made potentiostat and a Tacussel GSTP4 waveform generator. The voltammograms were recorded with a Nicolet 301 oscilloscope.

Materials: Toluene was distilled from sodium and acetonitrile was filtered through dry alumina. $[\text{Cu}(5\text{-}t\text{Bu-Sal})_2]$ (**1**) was prepared as described previously.^[12] Oxo ester **2** and methyl vinyl ketone (**3**) were commercial.

General Procedure for the UV/Vis Experiments: The UV/Vis experiments were performed in a 1 cm pathlength cell thermostatted at 30 °C. A solution of **1** (3 mL, 0.703 mM) in toluene was added to the cell. The UV/Vis spectroscopy was performed from time to time up to 20 h to test the stability of **1**. In another experiment, **2** (17.7 μL , 0.12 mmol, 20 equiv.) and **3** (48 μL , 0.6 mmol, 100 equiv.) were simultaneously added to the cell containing a fresh solution of **1** (3 mL, 2 mM) in toluene. The UV/Vis spectroscopy was performed from time to time up to 5 h (Figure 2) corresponding to the end of the catalytic reaction.

Kinetic Studies: The kinetics of the reaction of **1** (0.7 mM) with **2** was performed by recording the decrease in the absorbance of **1** at 397 nm with time after the addition of various amounts of **2** (20, 30, 40, and 50 equiv.) until total conversion in all cases. The decelerating effect of **6** (5 and 10 equiv.) on the rate of the reaction of **2** (20 equiv.) with **1** (0.25 mM) was investigated under the same conditions as above.

General Procedure for the Cyclic Voltammetry Experiments: Typical experiments were carried out in a three-electrode cell connected to a Schlenk line. The counter-electrode was a platinum wire of around 1 cm² apparent surface area. The reference was a saturated calomel electrode separated from the solution by a bridge filled with acetonitrile (2 mL) containing *n*Bu₄NBF₄ (0.3 M). Degassed acetonitrile (10 mL) containing *n*Bu₄NBF₄ (0.3 M) was introduced into the cell followed by **1** (8.3 mg, 0.02 mmol). Cyclic voltammetry was performed at a steady gold disk electrode (1 mm diameter) at a scan rate of 0.5 V s⁻¹ at 22 °C. The oxo ester **2** (3 μL , 0.02 mmol) was then added and cyclic voltammetry performed as above. The oxo ester **2** was then successively added up to 20 equiv. (see text) and CVs were recorded between two additions. In another experiment, complex **5** was generated by the reaction of the oxo ester **2** (12 μL , 0.08 mmol) with **1** (8.3 mg, 0.02 mmol). Methyl vinyl ketone (**3**; 1.6 μL , 0.02 mmol) was then added. Cyclic voltammetry was performed as above. Additional **3** (4.8 μL , 0.03 mmol) was finally added and monitored by CV.

Acknowledgments

Financial support from the Ministerio de Ciencia e Innovación of Spain (Projects CTQ2008-05409-C02-01 and CTQ2005-04968-C02-01), the Consolider Ingenio 2010 (CSD2007-00006), and the DURSI-Generalitat de Catalunya (SGR 2005-00305 and SGR 2009-1441) are gratefully acknowledged. E. P. acknowledges the Ministerio de Educación y Ciencia (MEC) for a predoctoral fellowship. The Centre National de la Recherche (CNRS) and Ecole Normale Supérieure (ENS) are also thanked for financial support.

- [1] a) M. E. Jung, "Stabilized nucleophiles with electron-deficient alkenes and alkynes" in *Comprehensive Organic Synthesis* (Eds.: M. B. Trost, I. Fleming), Pergamon Press, Elmsford, NY, **1991**, vol. 4, chapter 1.1; b) P. Perlmutter in *Conjugate Addition Reactions in Organic Synthesis*, Pergamon Press, New York, **1992**.
 [2] a) J. Christoffers, *Eur. J. Org. Chem.* **1998**, 1259–1266; b) J. Christoffers, A. Baro, *Angew. Chem. Int. Ed.* **2003**, *42*, 1688–

- 1690; c) J. Comelles, M. Moreno-Mañas, A. Vallribera, *Arkivoc* **2005**, 9, 207–238.
- [3] a) T. Saegusa, Y. Ito, S. Tomita, H. Kinoshita, *Bull. Chem. Soc. Jpn.* **1972**, 45, 496–499.
- [4] a) P. N. Howells, J. W. Kenney, J. H. Nelson, R. A. Henry, *Inorg. Chem.* **1976**, 15, 124–129; b) R. P. Eckberg, R. A. Henry, L. W. Cary, J. H. Nelson, *Inorg. Chem.* **1977**, 16, 2977–2979.
- [5] a) J. Christoffers, A. Mann, *Angew. Chem. Int. Ed.* **2000**, 39, 2752–2754; b) J. Christoffers, H. Schar, *Eur. J. Org. Chem.* **2002**, 1505–1508; c) J. Christoffers, K. Schuster, *Chirality* **2003**, 15, 777–782; J. Christoffers, *Chem. Eur. J.* **2003**, 9, 4862–4867; d) B. Kreidler, A. Baro, J. Christoffers, *Eur. J. Org. Chem.* **2005**, 5339–5348.
- [6] a) M. Marigo, K. Juhl, K. A. Jørgensen, *Angew. Chem. Int. Ed.* **2003**, 42, 1367–1369; b) N. Halland, T. Velgaard, K. A. Jørgensen, *J. Org. Chem.* **2003**, 68, 5067–5074; c) M. Marigo, N. Kumaragurubaran, K. A. Jørgensen, *Synthesis* **2005**, 957–960.
- [7] C. Palomo, M. Oiarbide, J. M. García, P. Bañuelos, J. M. Odriozola, J. Razkin, A. Linden, *Org. Lett.* **2008**, 10, 2637–2640.
- [8] J. S. Yadav, B. V. S. Reddy, G. Baishya, A. V. Narsaiah, *Chem. Lett.* **2005**, 34, 102–103.
- [9] J. Clariana, N. Gálvez, C. Marchi, M. Moreno-Mañas, A. Vallribera, E. Molins, *Tetrahedron* **1999**, 55, 7331–7344.
- [10] M. Meseguer, M. Moreno-Mañas, A. Vallribera, *Tetrahedron Lett.* **2000**, 41, 4093–4095.
- [11] C. Marchi, E. Trepát, M. Moreno-Mañas, A. Vallribera, E. Molins, *Tetrahedron* **2002**, 58, 5699–5708.
- [12] J. Comelles, M. Moreno-Mañas, E. Pérez, A. Roglans, R. M. Sebastián, A. Vallribera, *J. Org. Chem.* **2004**, 69, 6834–6842.
- [13] The value of $k^{\text{II}}_{\text{obs}}$ did not significantly vary with the concentration of **2**. $k^{\text{II}}_{\text{obs}} = 0.023, 0.037, 0.021$ and 0.029 s^{-1} for $[\mathbf{2}] = 0.014, 0.02, 0.023$ and 0.032 M , respectively, attesting to a zero-order reaction for the oxo ester **2** with an average value: $k^{\text{II}} = 0.028(\pm 0.007) \text{ s}^{-1}$ (toluene, 30 °C).
- [14] For a review of the use of cyclic voltammetry to investigate the mechanism of transition-metal-catalyzed reactions, see: A. Jutand, *Chem. Rev.* **2008**, 108, 2300–2347.
- [15] J. Comelles, A. Pericas, M. Moreno-Mañas, A. Vallribera, G. Drudis-Solé, A. Lledós, T. Parella, A. Roglans, S. Garcia-Granda, L. Rocés-Fernández, *J. Org. Chem.* **2007**, 72, 2077–2087.

Received: October 6, 2009
Published Online: January 28, 2010